Polyhedron 266 (2025) 117257

Contents lists available at ScienceDirect

Polyhedron

journal homepage: www.elsevier.com/locate/poly

Magnesium 4, 5, and 6 coordinate complexes with ligands bound via sp or sp^2 hybridized atoms

Annabel Rae, Alan R. Kennedy, Stuart D. Robertson *

WestCHEM, Department of Pure and Applied Chemistry, University of Strathclyde, Glasgow G1 1XL, UK

ARTICLE INFO

Dedicated to Prof Robert Mulvey in celebration of his 65th birthday, with thanks for many years of mentorship, and more importantly friendship. *Hail Hail!*

Keywords:
Magnesium
Molecular Structure
NMR spectroscopy
Imide

ABSTRACT

As a metallic element of high natural abundance, magnesium finds a wide range of uses in both stoichiometric and more recently catalytic applications. This often takes advantage of the basic or nucleophilic properties of its compounds or their ability to co-complex with other organometallic compounds. However, the homoleptic chemistry of Mg(II) is heavily skewed towards alkyl and aryl ligands bound via sp^2 and sp^3 hybridized atoms. Here, we report our combined NMR spectroscopic and X-ray crystallographic study into much rarer alternative THF solvates of homoleptic magnesium complexes using ligands which bind via sp (alkynyl) and sp^2 (imido) atoms. Specifically, we exploit the high acidity of terminal alkynes and diphenylacetonitrile to prepare tetra-solvated distorted octahedral complexes $Mg(C{\equiv}CC_6H_4R\text{-}p)_2(THF)_4$ (R = Me, CF_3) and $Mg(N{=}C{=}CPh_2)_2(THF)_4$ starting from the commercial alkyl reagent $MgBu_2$. Adopting a similar deprotonative strategy using benzophenoneimine $Ph_2C{=}NH$ affords the heteroleptic trinuclear complex $Mg_3(N{=}CPh_2)_4nBu_2(THF)_2$ with distorted tetrahedral Mg centres. Related imidomagnesium halide complexes can be accessed either by deprotonation of the imine with a Grignard reagent, or nucleophilic addition of a Grignard reagent to a nitrile, but these unusual five-coordinate complexes are unresponsive to a 1,4-dioxane induced Schlenk equilibrium shift. Employing a higher reflux temperature switching from a THF to a toluene medium permits access to the THF solvate of a homoleptic imido complex which also possesses a trinuclear constitution in $Mg_3(N{=}CPh_2)_6(THF)_2$.

1. Introduction

In recent work, we disclosed a 100 % atom economic synthetic protocol to access the All-Phenyl Complex (APC, Eq. (1)) [1], a magnesium aluminate of formula $[Mg_2Cl_3]^+[AlPh_4]^-$ which is currently one of the leading electrolyte complexes (when dissolved in and solvated by THF) in magnesium battery research [2].

$$AlCl_3 + 2\ MgPh_2 \xrightarrow{THF} \underset{\text{'APC'}}{[Mg_2Cl_3{\cdot}6THF]^+[AlPh_4]^-} \quad \textbf{(eq. 1)}$$

This reaction involved ligand exchange of two molar equivalents of homoleptic diarylmagnesium with $AlCl_3$ (we use the term homoleptic in this context here, and throughout this manuscript, to define a complex RMgR' where R = R', i.e. with respect to the anionic ligands attached to the divalent metal without including any Lewis donor solvents which may also be present). While other ligands notably alkyls have also been studied in this context, the phenyl group is preferable on account of its diminished nucleophilicity versus a sp^3 hybridized carbanion and the lack of a beta-hydride elimination decomposition pathway, making it a more robust electrolyte, for example being less susceptible to problematic side-reactions with electrodes. With this protocol to hand, the potential now exists to access a greater range of magnesium aluminate electrolytes, provided suitable homoleptic diorganomagnesium starting materials are available. Given the success of the sp^2 hybridized phenyl group in the APC for the aforementioned reasons, we reasoned that other ligands based on sp^2, or indeed sp hybridized atoms might exhibit similar promise in this domain. The ketimide ($^-N{=}CR_2$) and alkynyl ($^-C{\equiv}CR$) ligand classes seemed ideally suited to this task given the ease with which such homoleptic complexes could be targeted, specifically by deprotonation of the relatively acidic parent proligand with a bis-alkyl magnesium base. Furthermore, ketimido-magnesium complexes have an alternative access route via nucleophilic addition of a Mg-C unit to the unsaturated N≡C bond of a nitrile, opening up the field further. Despite their expected simplicity of preparation, there are surprisingly few crystallographically verified solvates of homoleptic complexes of type $Mg(N{=}CR_2)_2$ or $Mg(C{\equiv}CR)_2$ reported in the literature. Incentivized

* Corresponding author.
E-mail address: stuart.d.robertson@strath.ac.uk (S.D. Robertson).

https://doi.org/10.1016/j.poly.2024.117257
Received 21 August 2024; Accepted 7 October 2024
Available online 24 October 2024

by this paucity of such examples, as reported herein we pursued the synthesis and characterization of such complexes, targeting facile synthetic approaches (that is those requiring minimal steps) with easily accessible starting materials to ensure the viability of any future onward reactions.

2. Results and discussion

2.1. sp hybridized anions

For consistency throughout our study, we decided to utilize aryl substituted ligands and target only THF solvates, as any future electrolytic use will likely take place in ethereal solution as is customary currently in the field of Mg batteries [3,4]. While a handful of bis(alkynyl)magnesium complexes can be found in the literature, most are not supported by THF solvation. Hill serendipitously synthesised a polymeric $Mg(C{\equiv}CPh)_2$ complex containing bridging alkynyl ligands with every third Mg centre solvated by two THF molecules making them 6-coordinate, whereas the preceding two centres are unsolvated and only 4-coordinate [5]. Coles then reported a monomeric variant, on reacting $MgBu_2$ with two equivalents of alkyne in THF [6]. This complex also contains a 6-coordinate Mg centre with the alkynyl ligands disposed trans to one another and four THF solvate molecules filling the equatorial plane. This structure mirrors the only other THF solvated bis(alkynyl)magnesium complex reported, which utilized triphenylsilylacetylide $Ph_3SiC{\equiv}C^-$ as the organic ligand. We adopted this deprotonative approach, using the *p*-Me and *p*-CF_3 substituted arylacetylenes to allow comparison of electron donating and electron withdrawing groups substituted on the phenyl ring (Eq. (2)).

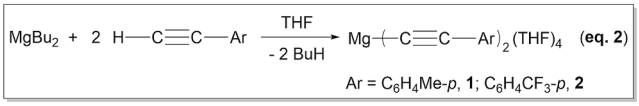

Reactions were carried out in THF solution and cooling to −36 °C for a week produced X-ray Diffraction (XRD) quality crystals, whose molecular structures (Figs. 1 and 2) confirmed isostructural arrangements for $Mg(C{\equiv}CC_6H_4Me\text{-}p)_2(THF)_4$ (**1**) and $Mg(C{\equiv}CC_6H_4CF_3\text{-}p)_2(THF)_4$ (**2**). Specifically, the anionic alkynyl ligands lie trans to one another with four neutral THF molecules again occupying the equatorial plane. Table 1 provides a comparison of some pertinent bond parameters alongside those of the non-substituted phenylacetylide complex as reported by Coles [6].

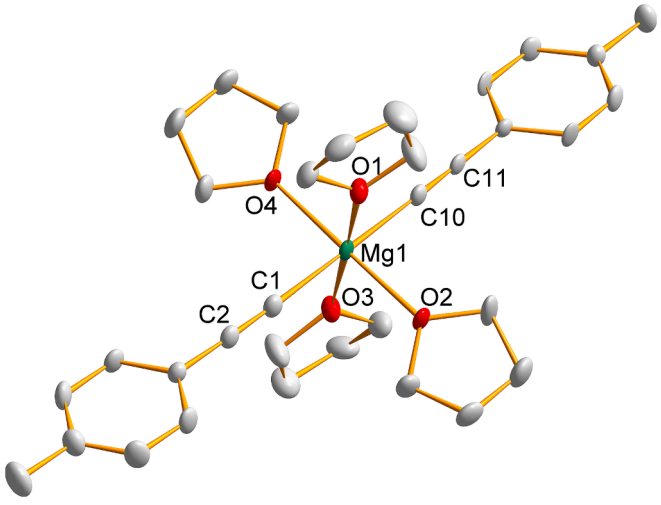

Fig. 1. Molecular structure of $Mg(C{\equiv}CC_6H_4Me\text{-}p)_2(THF)_4$ (**1**) showing atom labelling with ellipsoids drawn at 50 % probability and disordered THF molecule and hydrogen atoms removed for clarity.

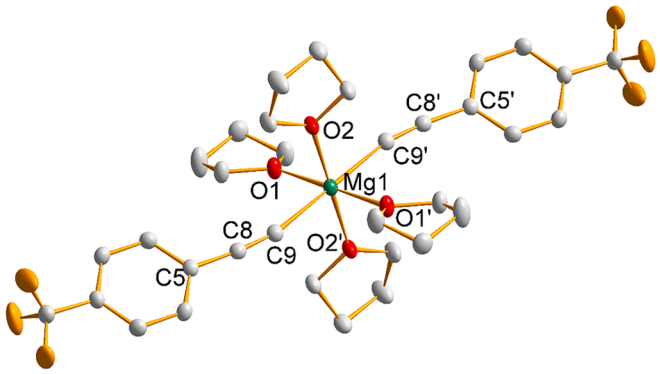

Fig. 2. Molecular structure of $Mg(C{\equiv}CC_6H_4CF_3\text{-}p)_2(THF)_4$ (**2**) showing atom labelling with ellipsoids drawn at 50% probability and disordered components and hydrogen atoms removed for clarity. Symmetry operation to generate atoms denoted ‘: −x, 2-y, −z.

Table 1
Comparative selected bond distances (Å) and angles (°) of bis(alkynyl)magnesium $Mg(C{\equiv}CC_6H_4R\text{-}p)_2(THF)_4$ complexes.

	R = H	R = Me (**1**)	R = CF_3 (**2**)
Mg-C	2.187(2); 2.191(2)	2.188(2); 2.180(2)	2.224(1)
Mg-O	2.190(1); 2.230(1)	2.182(2); 2.210(2)	2.177(1)
		2.176(2); 2.204(2)	2.172(1)
C≡C	1.224(3); 1.220(3)	1.231(3); 1.220(3)	1.225(2)
C-Ph	1.435(3); 1.442(3)	1.442(3); 1.437(3)	1.440(2)
O-Mg-C	89.03(3)–90.97(3)	89.21(7)–91.46(7)	88.52(4)–91.48(4)
O-Mg-O_{cis}	89.91(5)–90.11(5)	86.74(7)–92.44(7)	87.25(4); 92.75(4)
O-Mg-O_{trans}	180	178.49(7); 178.86(7)	180
C-Mg-C	180	178.93(9)	180
Mg-C≡C	180	175.9(2); 177.1(2)	167.0(1)
C≡C-Ar	180	178.2(2); 178.7(2)	171.0(2)

Unsurprisingly, there are many similarities between the bond metrics of these three octahedral, isostructural complexes. The largest difference is in the deviation from linearity of the alkynyl ligands in the fluorinated derivative **2**, evident in the Mg-C≡C and C≡C-Ar bond angles, with the unsubstituted complex having crystallographically imposed angles of 180° and complex **1** deviating only slightly, with the largest deviation being Mg-C≡C at 175.9(2)°. However, in complex **2**, this bending is considerably more pronounced at 167.0(1) and 171.0(2)° for the Mg-C≡C and C≡C-Ar bond angles, which may be caused by intermolecular interaction between C8 of the alkynyl ligand and the C15 sites of a disordered THF fragment of a neighbouring molecule (C-H = 2.67 Å).

Unlike Coles *et al.* for $Mg(C{\equiv}CPh)_2(THF)_4$, we were able to identify the alkynyl resonances in the ^{13}C NMR spectra of **1** and **2** in THF-d_8 at 133.9/139.4, and 108.6/108.1 ppm for the aryl and metal bound sp carbon atoms respectively. Interestingly, the ^{13}C spectrum of **2** was slightly more difficult to assign due to the coupling of the fluorine to the CF_3, *meta* and *para* carbons splitting these peaks into quartets (Fig. 3). Only the internal two resonances of the 1:3:3:1 quartet for the *para* and CF_3 carbons were seen due to the low resolution of the outer two resonances (this could not be improved with an increased concentrated of sample, with the outer resonances still hidden within the signal:noise ratio of the baseline). Specifically, we witnessed CF coupling constants of 271.38, 32.07 and 3.85 Hz for the ^1J (blue), ^2J (green) and ^3J (red) coupling. These values mirror closely those of the parent alkyne in $CDCl_3$ with corresponding coupling constants of 273, 32.8 and 3.8 Hz respectively [7]. A singlet at −63 ppm in the ^{19}F NMR spectrum was evident for the CF_3 group in **2**.

2.2. sp^2 hybridized anions

Moving to the use of ligands which bind via sp^2 hybridized atoms, we

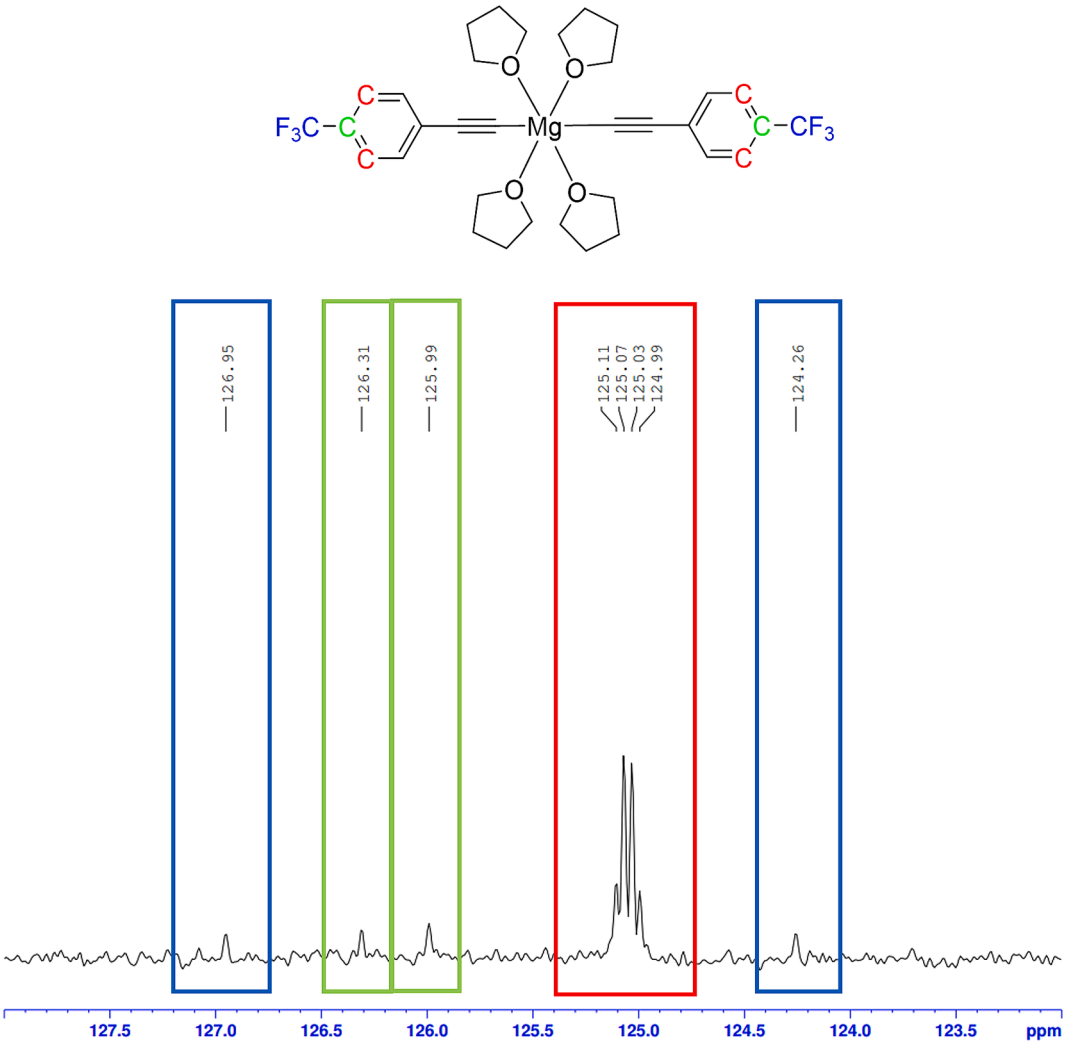

Fig. 3. Section of ^{13}C NMR spectrum of complex **2** in THF-d_8 showing coupled resonances.

first considered diphenylacetonitrile, which can be deprotonated at the diaryl substituted carbon centre with the resulting negative charge transferred to the terminal nitrogen via tautomerisation resulting in a ketinimide $Ph_2C{=}C{=}N^-$ anion (Eq. 3).

$$MgBu_2 + 2\ N{\equiv}C{-}C(H)Ph_2 \xrightarrow[-\ 2\ BuH]{THF} \underset{\mathbf{3}}{Mg{-}(N{=}C{=}CPh_2)_2(THF)_4} \quad \textbf{(eq. 3)}$$

Surprisingly, we are only aware of three structurally verified group two ketinimide fragments, two reported by Fedushkin *et al.*, both of which are heteroleptic bis(imino)acenaphthene complexes (M = Mg [8], Ba [9]), and one by Hill *et al.* of a dinuclear Mg(nacnac) borate [10], but both Hevia [11] and ourselves [12] have recently demonstrated that a *N*-heterocyclic carbene can deprotonate this substrate, with these combined reports giving us confidence that a homoleptic magnesium complex is accessible from $MgBu_2$. Indeed, this proved to be the case at room temperature in a hexane/THF mixture. Additional THF was required to fully dissolve all precipitate resulting in XRD quality crystals of $Mg(N{=}C{=}CPh_2)_2(THF)_4$, (**3**) growing after 2 days at 5 °C. Mimicking complexes **1** and **2**, complex **3** (Fig. 4) contains a distorted octahedral magnesium centre with the two anionic ketinimido ligands lying trans to one another and four THF molecules occupying the equatorial plane. While the constitution of complex **3** could be clearly ascertained, the quality of the data precluded a detailed bond analysis.

The solution NMR data in d_8-THF are consistent with the solid-state structure, specifically the ^{13}C NMR resonances of the C=C unit, displaying resonances at 143.9 and 53.2 ppm for the *N*-bound and Ph-bound carbon atoms respectively. These chemical shifts closely mirror those of Hevia's gallium complex (143.4 and 55.7 ppm, respectively) [11].

Next, we targeted some bis(imido)magnesium complexes, repeating the deprotonation approach using commercial benzophenoneimine as substrate. While imido complexes of the alkali metals have been widely studied [13,14], leading to the development of the ring-stacking concept by Mulvey, Snaith and Wade [15,16], there are surprisingly few homoleptic bis(imido)magnesium complexes reported in the literature [17–19], with the closest example perhaps Mulvey's bimetallic $Na_2Mg_2(NCPh_2)_6$, formed by the deprotonative action of a $NaBu/MgBu_2$ bimetallic base upon three molar equivalents of the parent imine [20]. We reacted two equivalents of benzophenoneimine with $MgBu_2$ in THF/hexane (Eq. (4)) obtaining a precipitate which could be redissolved with addition of further THF and recrystallized at low temperature. XRD analysis on a single crystal of this product showed it to be a trinuclear heteroleptic complex of formula $Mg_3(N{=}CPh_2)_4nBu_2(THF)_2$ (**4**, Fig. 5). Its central magnesium centre is tetracoordinated by imido ligands which bridge to the outer Mg atoms to give a spirocyclic Mg_3N_4 core. The outer magnesium atoms are also four-coordinate, completed by a terminal *n*Bu anion and solvating THF molecule. This complex could thus be considered to consist of a central homoleptic $Mg(imide)_2$ molecule co-complexed to a pair of *n*BuMg(imide)(THF) molecules.

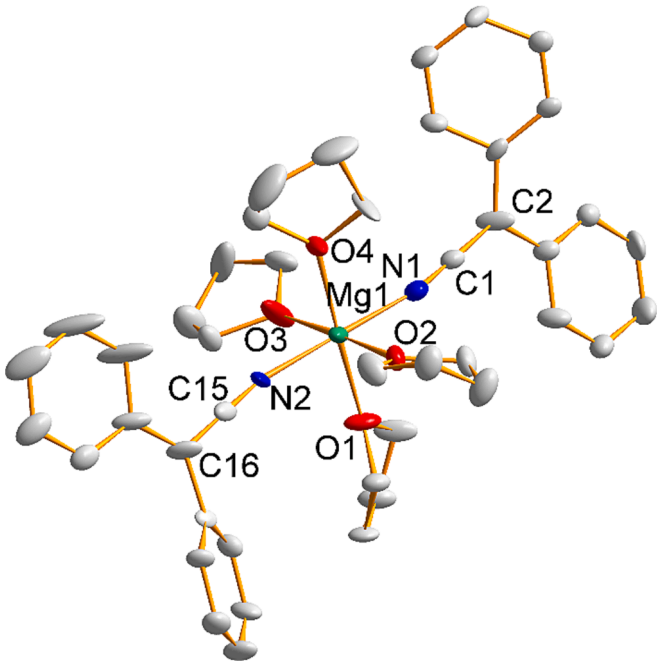

Fig. 4. Molecular structure of $Mg(N{=}C{=}CPh_2)_2(THF)_4$ (**3**) showing atom labelling with ellipsoids drawn at 50 % probability and disordered components and hydrogen atoms removed for clarity.

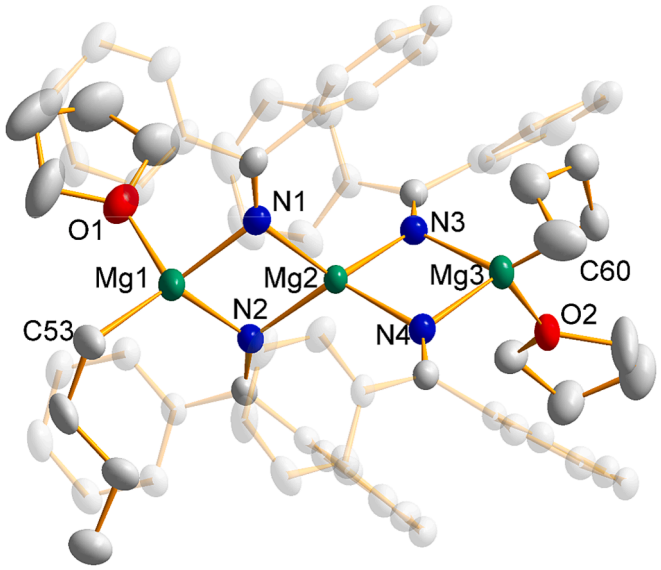

Fig. 5. Molecular structure of $Mg_3(N{=}CPh_2)_4nBu_2(THF)_2$ (**4**) showing atom labelling with ellipsoids drawn at 50 % probability and disordered *n*Bu, THF molecule of crystallization and hydrogen atoms removed for clarity.

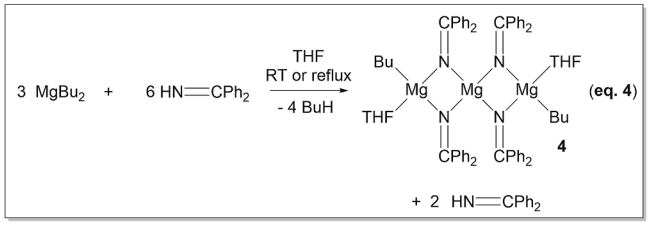

The central Mg(2) is in a distorted tetrahedral environment as a consequence of the constraints imposed by the four-membered Mg_2N_2 rings with those endocyclic angles held at 86.20(7)/86.77(7)° while the exocyclic N-Mg-N angles average 122.0°. The eight Mg-N bonds span the narrow range 2.085(2)–2.120(2) Å, consistent with the Mg_2N_2 ring located centrally in Mulvey's complex [2.113(1) Å]. The constraints imposed by the four-membered ring also distort the outer magnesium atoms from tetrahedral although the terminal ligands revert to near tetrahedral positions, lying at 106.85(13)/102.86(9)° for Mg1 and Mg3 respectively. This spirocyclic motif is unusual but not unprecedented, with Power having reported amide bridges in $Mg_3(NHDipp)_4(HMDS)_2$ [21]. formed by deprotonation of the primary amine H_2NDipp via $Mg(HMDS)_2$ (Dipp = 2,6-diisopropylphenyl; HMDS = 1,1,1,3,3,3-hexamethyldisilazide), although the considerable bulk of the HMDS anions precluded THF coordination. Stephan prepared the homoleptic phosphinimide complex $[Mg_3(N{=}PiPr_3)_6]$ by deprotonation of the parent phosphinimine with $MgBu_2$ [22]. Again, this has three-coordinate outer magnesium centres, consistent with the bulk of the phosphinimide ligands. Bulkier phosphinimide ligands reduce the aggregation, with *t*Bu groups resulting in a dinuclear $Mg_2(N{=}PtBu_3)_4$ complex. Note that we previously reported an oligomeric spirocyclic structure for the parent magnesium base in the form of $Mg_4nBu_8(IPr)_2$ (IPr = 1,3-bis-(2,6-diisopropylphenyl)imidazol-2-ylidene) [23] which perhaps suggests that organomagnesium complexes are predisposed to forming structures such as **4** wherever possible.

In solution, the ^1H NMR spectrum in THF-d_8 revealed the presence of phenyl rings and *n*-butyl ligands in the expected 8:2 ratio, with the Mg-bound CH_2 group being particularly diagnostic, appearing as a heavily shielded resonance at −1.24 ppm. This was mirrored in the ^{13}C NMR spectrum, appearing as the most shielded resonance at 10.7 ppm, while the diagnostic C=N functionality resonated at 176.5 ppm, again similar to that in Mulvey's heterometallic magnesium imide (178.5 ppm) [20].

Refluxing the $MgBu_2/Ph_2C{=}NH$ mixture in THF resulted in the same heteroleptic complex **4** being obtained. Thus, with no homoleptic complex to hand we devised the alternative synthetic strategy of forming a heteroleptic imido magnesium halide complex [$(R_2C{=}N)MgX$] and then converting it into a homoleptic complex by manipulation of the Schlenk equilibrium [24,25]. We identified two potential routes to the original pseudo-Grignard complex, either through direct deprotonation of the imine with a more basic Grignard reagent or by the nucleophilic addition of a Grignard reagent to an organic nitrile (scheme 1). The

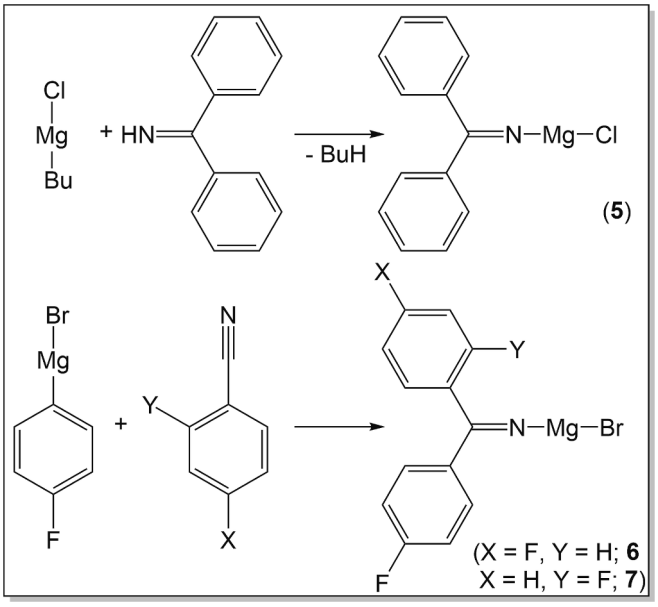

Scheme 1. Deprotonation (top) and nucleophilic addition (bottom) methods to imido magnesium halide (pseudo-Grignard reagent) complexes **5**–**7** (note only empirical formulae shown).

Grignard addition to a nitrile is a well-established methodology for imine synthesis [26], primarily as a means of generating a precursor on the route to ketones, but there is a paucity of knowledge regarding the molecular structures of such halomagnesium imido intermediates, *vide infra*. This route introduced the additional flexibility of generating a non-symmetrical imide, since the two groups bound to the imido sp^2 carbon atom come from different sources, one from the Grignard reagent and the other from the nitrile.

Both routes proved successful in hot THF solution, giving crystalline material upon cooling in reasonable yield in both instances. For the deprotonation route, benzophenoneimine was again used as the substrate to access complex **5**; whereas for the addition route, *para*-fluorophenylmagnesium bromide and *para*-fluorobenzonitrile were chosen to access complex **6**. This reaction was utilized previously to generate complex **6** *in situ* but rather than being isolated it was quenched immediately to yield the fluorinated benzophenoneimine [27]. To demonstrate the applicability of this route towards non-symmetric imides, *ortho*-fluorobenzonitrile was also used, yielding complex **7**. Isostructural complexes were obtained in all three cases. For brevity, only the structure of complex **6** is shown (Fig. 6), with those of **5** and **7** available in the Supporting Information, while Table 2 compares selected bond parameters.

These are THF-solvated dinuclear complexes with the magnesium centres in the unusual coordination number of five. The imido ligands act as bridges while the halides are terminal, with a terminal THF molecule on each magnesium and also a bridging THF molecule spanning the two metals. These structures represent rare examples of imidomagnesium halides, the closest example to those here being that of Charette *et al.*, who took an addition approach of MeMgBr to an alkoxynitrile, although in this example the smaller steric profile of the methyl groups permitted two THF molecules per Mg which when coupled with intramolecular alkoxy coordination resulted in a more common six-coordinate octahedral metal centre [28]. Clot, Gade *et al.* have reported an octameric example containing a central cubane-type motif obtained via the nitrile addition route [29], while Semeniuchenko and Johnson applied the deprotonation route to access dimeric complexes akin to **5** and **6** but without the bridging THF molecule, where the imine was derived from (1-methylpyridin-4(1*H*)-ylidene)amide [19]. Davidson *et al.* have exploited the deprotonation methodology using $HN{=}PPh_3$ to obtain dimeric, HMPA solvated complexes again containing four-coordinate magnesium cations [30].

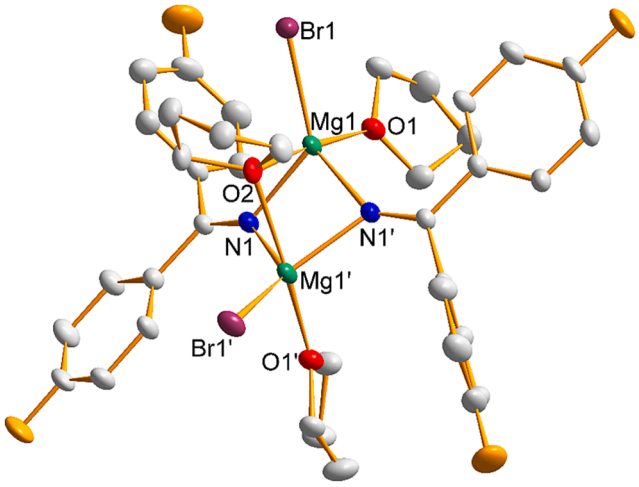

Fig. 6. Molecular structure of $[(p\text{-}FC_6H_4)_2C{=}NMgBr]_2(THF)_3$ (**6**) showing atom labelling with ellipsoids drawn at 50 % probability and disordered THF and hydrogen atoms removed for clarity. Symmetry operation to generate atoms denoted ': 1 − x, y, 0.5 − z.

As already mentioned, the Mg centres are coordinated by five ligands resulting in distorted trigonal bipyramidal geometries for each. The neutral THF ligands can be considered as lying in the axial positions [O-Mg-O angles of 172.85(5)/173.27(6)/175.8(1)° for **5**–**7** respectively] leaving the bridging imido anions and terminal halides to occupy the equatorial sites although these are distorted from planarity in each case with the sum of the equatorial angles being 349.55/349.63/350.5° respectively. This deformation can be in part explained by the strain imposed by the four-membered $[MgN]_2$ ring which itself is folded rather than planar, particularly so for the complex with the lighter halide [Σ < = 341.14/351.90/350.8°]. The double bond character of the CN units is reflected by their 1.265(3)/1.266(3)/1.253(5)Å lengths while the THF bridge is unsurprisingly longer at 2.382(2)/2.351(2)/2.334(3)Å versus the terminal THF at 2.053(1)/2.052(2)/2.060(3)Å.

In solution, the ^1H and ^{13}C NMR spectra of **5** confirm the presence of the benzophenoneimide anion but are otherwise unremarkable. Reduction of the nitrile triple bond in the formation of **6** is evident via replacement of the C≡N resonance at about 118 ppm [31] with a C=N resonance at 172 ppm. Its ^{19}F NMR spectrum displays a singlet at −114.1 ppm, close to the value of the parent imine at −109.8 ppm (albeit in $CDCl_3$ [32], and shifted from the resonance of the nitrile starting material (−103.0 ppm) [33]. Likewise, the most important resonance of complex **7** is that of the C=N imide unit at 167.1 ppm. Interestingly, while the ^{19}F NMR spectrum displays two equal intensity resonances as expected, at −113.3 and −117.3 ppm, the more shielded resonance is clearly split into a broad doublet. Variable temperature NMR spectroscopy (see Fig. S23) shows this to coalesce at 305 K before forming a sharp singlet at higher temperatures. This is potentially a consequence of rotation around the C-Ar bond of the *ortho*-substituted aromatic ring. If viewed from an alternative angle (Fig. S31), this ring lies approximately perpendicular to the Mg_2N_2 ring, with the *ortho* fluoro group (green) pointing downwards, that is '*cis*' to the terminal THF molecules and '*trans*' to the Br ligands (Fig. 7, left). 180° rotation of the C-Ar would leave the F atoms in an inequivalent position, now '*trans*' to the terminal THF molecules and '*cis*' to the Br ligands, resulting in magnetic inequivalence of these two positions and hence displaying separate resonances.

Using $\Delta G^{\ddagger} = RT_c[22.96 + \ln(T_c/\Delta\nu)]$, derived from the Eyring

Table 2
Selected bond distances (Å) and angles (°) of (imido)magnesium halide complexes **5**–**7**.

	X = Cl (**5**)	X = Br (**6**)	X = Br (**7**)		X = Cl (**5**)	X = Br (**6**)	X = Br (**7**)
Mg1-O1	2.053(1)	2.052(2)	2.060(3)	O1-Mg1-O2	172.85(5)	173.27(6)	175.8(1)
Mg1-O2	2.382(2)	2.351(2)	2.334(3)	O1-Mg1-X1	97.60(5)	96.18(6)	95.7(1)
Mg1-X1	2.316(1)	2.480(1)	2.488(2)	O1-Mg1-N1	99.09(7)	107.44(8)	104.1(2)
Mg1-N1	2.086(2)	2.089(2)	2.098(4)	O1-Mg1-N1′	105.66(6)	99.00(7)	101.2(2)
Mg1-N1′	2.089(2)	2.084(2)	2.078(4)	O2-Mg1-X1	88.05(2)	87.27(2)	87.93(5)
N1-C1	1.265(3)	1.266(3)	1.253(5)	O2-Mg1-N1	73.82(5)	74.33(6)	74.6(1)
				O2-Mg1-N1′	73.77(5)	74.43(6)	74.9(1)
Mg1-N1-Mg1′	81.21(7)	86.71(8)	86.6(2)	X1-Mg1-N1	131.74(6)	129.66(6)	133.8(1)
Mg1-N1-C1	141.4(2)	129.9(2)	129.8(3)	X1-Mg1-N1′	128.45(5)	130.73(6)	127.9(1)
Mg1′-N1-C1	129.2(2)	142.9(2)	143.4(3)	N1-Mg1-N1′	89.36(7)	89.24(8)	88.8(2)

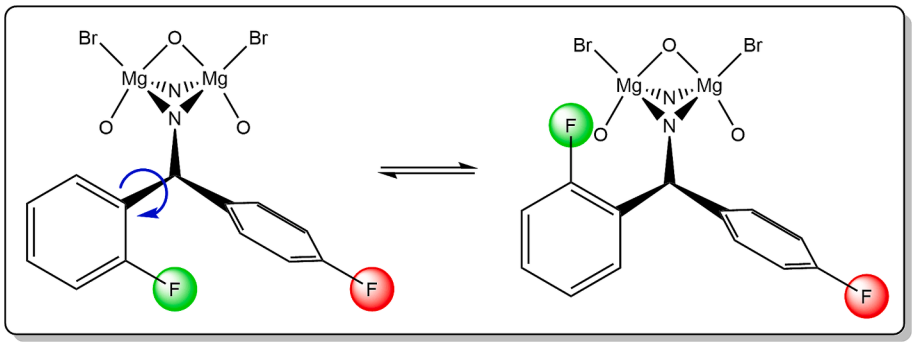

Fig. 7. Showing potential magnetic inequivalence of green fluorine atom due to C-C rotation (O = neutral THF molecule).

equation, allows a reasonable estimate at the energy barrier for this equilibrium [34]. With a coalescence temperature (T_c) of 305 K and a $\Delta\nu$ value of 287 Hz (the difference in chemical shift between the two singlets at low temperature; R is the gas constant 8.314 J K^{-1} mol^{-1}), we obtained a value of 58.37 kJ mol^{-1}.

Unfortunately, these three imidomagnesium halide complexes were unresponsive to 1,4-dioxane, that is that addition of this solvent failed to shift the Schlenk equilibrium [35] to the right, precipitating MgX_2 and leaving behind the target homoleptic complex in solution. Therefore, we reverted to deprotonating the parent imine with $MgBu_2$, but altered the solvent to toluene so that we could access higher temperatures trusting that the terminal butyl groups of complex **4** could be induced to react (Eq. 5). This proved correct, since a $MgBu_2$ and benzophenoneimine (1:2) reaction in refluxing toluene yielded red crystals of $Mg_3(N{=}CPh_2)_6(THF)_2$, (**8,** Fig. 8) which showed that though the trinuclear arrangement had been retained, a homoleptic complex was formed.

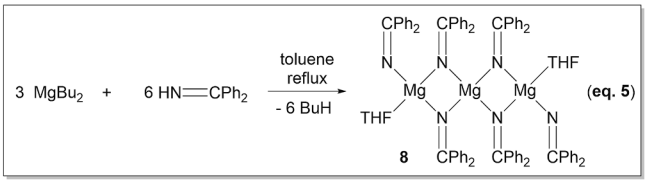

With an identical $Mg_3L_6(THF)_2$ motif to **4**, the metrics of the core $M_3(imido)_4$ fragments are as expected similar as can be ascertained from Table 3. The terminal butyl ligands have now been replaced with terminal imido ligands which are bound in a bent fashion [average Mg-N=C bond angle = 152.1°] reflecting the sp^2 nature of the terminal ligand. These terminal ligands unsurprisingly display shorter Mg-N bonds [average 1.960 Å] than those forming the bridges [average 2.082 Å].

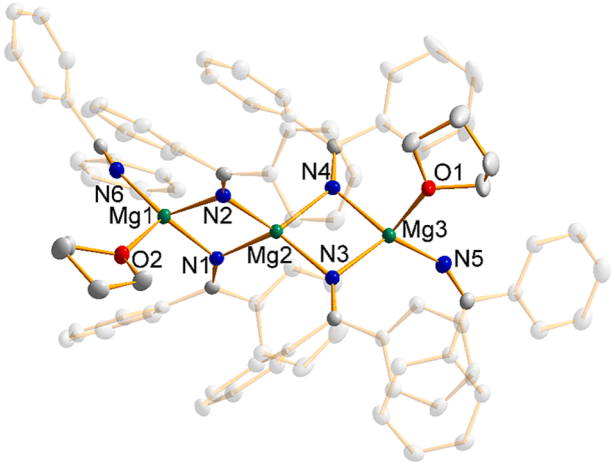

Fig. 8. Molecular structure of $Mg_3(N{=}CPh_2)_6(THF)_2$ (**8**) showing atom labelling with ellipsoids drawn at 50 % probability and toluene molecule of crystallization and hydrogen atoms removed for clarity.

Table 3
Selected bond distances (Å) and angles (°) of trinuclear (imido)magnesium complexes **4** and **8.**

	4	**8**		**4**	**8**
Mg1-O1	2.028(2)	2.045(1)	N1-Mg1-N2	86.00(7)	87.20(6)
Mg1-N6	–	1.967(1)	N1-Mg1-O1	95.16(8)	116.03(6)
Mg1-C53	2.158(4)	–	N1-Mg1-N6	–	122.67(6)
Mg1-N1	2.090(2)	2.071(1)	N1-Mg1-C53	130.20(11)	–
Mg1-N2	2.120(2)	2.102(1)	N2-Mg1-O1	113.03(8)	97.75(5)
Mg2-N1	2.090(1)	2.066(1)	N2-Mg1-N6	–	126.05(6)
Mg2-N2	2.090(2)	2.095(1)	N2-Mg1-C53	122.31(12)	–
Mg2-N3	2.101(2)	2.069(1)	O1-Mg1-N6	–	104.90(6)
Mg2-N4	2.085(2)	2.080(1)	O1-Mg1-C53	106.85(13)	–
Mg3-N3	2.118(2)	2.084(1)	N1-Mg2-N2	86.77(7)	87.53(6)
Mg3-N4	2.101(2)	2.086(1)	N1-Mg2-N3	122.72(7)	122.61(6)
Mg3-N5	–	1.954(2)	N1-Mg2-N4	122.43(7)	121.40(6)
Mg3-C60	2.163(3)	–	N2-Mg2-N3	120.98(7)	123.25(6)
Mg3-O2	2.057(1)	2.037(1)	N2-Mg2-N4	122.04(7)	117.97(6)
N1=C	1.265(3)	1.271(2)	N3-Mg2-N4	86.20(7)	87.88(6)
N2=C	1.269(3)	1.272(2)	N3-Mg3-N4	85.35(7)	87.33(6)
N3=C	1.264(3)	1.271(2)	N3-Mg3-O2	97.14(7)	116.61(6)
N4=C	1.272(3)	1.271(1)	N3-Mg3-N5	–	124.03(6)
N5=C	–	1.255(2)	N3-Mg3-C60	132.87(9)	–
N6=C	–	1.257(2)	N4-Mg3-O2	113.05(7)	101.03(6)
			N4-Mg3-N5	–	126.13(7)
			N4-Mg3-C60	123.16(9)	–
Mg1-N1-Mg2	93.86(7)	93.15(6)	O2-Mg3-N5	–	100.72(6)
Mg1-N2-Mg2	93.00(8)	91.42(6)	O2-Mg3-C60	102.86(9)	–
Mg2-N3-Mg3	93.47(7)	92.57(6)	Mg1-N6=C	–	152.2(1)
Mg2-N4-Mg3	94.42(7)	92.18(6)	Mg3-N5=C	–	152.0(1)

In THF-d_8 solution, it was clear that all the basic butyl groups had now been lost, with no resonances in the diagnostic Mg-CH_2 region of either the ^1H or ^{13}C spectrum such as seen for the putative precursor complex **4**. The mix now of both terminal and bridging imido ligands was reflected in the broadening of the aromatic resonances within the ^1H NMR spectrum, where no fine detail could now be observed, suggesting that complex **8** maintains its trinuclear form in solution.

In an attempt to disrupt the trinuclear framework, a pure sample of **7** was dissolved in toluene in the presence of two molar equivalents of the common bidentate donor TMEDA (*N,N,N',N'*-tetramethylethylenediamine, $Me_2NCH_2CH_2NMe_2$) with the solution cooled to −25 °C for a week. However, this resulted only in the recrystallisation of authentic **8**, demonstrating the robust nature of this THF-solvated trimetallic constitution.

3. Conclusions

Performed as a precursor to future magnesium battery studies, this

work has increased the number of known crystallographically characterized (THF-solvated) magnesium complexes containing ligands bound via sp or sp^2 hybridized atoms, revealing a variety of coordination numbers and geometries. Two new bis(alkynyl) complexes $Mg(C{\equiv}CC_6H_4R\text{-}p)_2(THF)_4$ (R = CH_3, CF_3) continue the trend of tetrasolvated octahedral complexes with *trans*-disposed alkynyl anions, a geometrical conformation also seen in the first bis(ketinimide) magnesium complex, $Mg(N{=}C{=}CPh_2)_2(THF)_4$. The benzophenoneimido magnesium complex $Mg_3(N{=}CPh_2)_6(THF)_2$ prefers a tetrahedral arrangement but aggregates into a trinuclear chain held together by imide bridges despite the presence of THF which typically deaggregates arrangements of this type. Such a complex could only be accessed from the deprotonation of the parent imine with $MgBu_2$ in refluxing toluene, with lower boiling point solvents resulting in incomplete deprotonation and generation of the heteroleptic imido/Bu trinuclear complex $Mg_3(N{=}CPh_2)_4nBu_2(THF)_2$. A family of imido magnesium halide complexes $[R^1R^2C{=}N]_2Mg_2X_2(THF)_3$ were also prepared, which revealed a consistent dimeric arrangement with the less common coordination number of five at magnesium, made up of bridging imides, terminal halides, and both terminal and bridging THF molecules. These complexes could be accessed either by direct deprotonation of an imine with an alkyl Grignard reagent ($R^1 = R^2$ = Ph; X = Cl), or through the nucleophilic addition of an aryl Grignard reagent to an arylnitrile ($R^1 = R^2 = p\text{-}FC_6H_4$; X = Br), with the latter route giving access to asymmetric imido anions ($R^1 = o\text{-}FC_6F_4$, $R^2 = p\text{-}FC_6H_4$; X = Br). However, it was found that none of these complexes react with 1,4-dioxane to shift the Schlenk equilibrium in favour of homoleptic bis(imido) and magnesium dihalide mixtures, leaving the deprotonation route in toluene as the sole current methodology for accessing such complexes.

4. Experimental section

4.1. General experimental

All reactions were performed under a protective argon atmosphere using standard Schlenk techniques. THF and toluene were degassed with nitrogen, dried over activated aluminium oxide (Innovative Technology, Pure Solv 400-4-MD, Solvent Purification System), and then stored under inert atmosphere over activated 4 Å molecular sieves. $MgBu_2$ (0.7 M in hexane with a small amount of THF), BuMgCl (2.0 M in THF), *p*-FC_6H_4MgBr, 4-methylphenylacetylene, 4-trifluoromethylphenylacetylene, diphenylacetonitrile, benzophenoneimine, *p*-fluorobenzonitrile and *o*-fluorobenzonitrile were obtained from commercial sources and used as received. THF-d_8 was degassed by freeze–pump–thaw methods and stored over activated 4 Å molecular sieves. ^1H, ^{13}C, and ^{19}F NMR spectra were recorded on a Bruker AV400 MHz spectrometer operating at 400.13, 100.62 and 376.46 MHz respectively.

All crystallographic measurements were made with monochromatic Cu radiation (λ = 1.54184 Å) using either an Oxford Diffraction Gemini-S diffractometer (complex **1**) or a Rigaku Synergy-i diffractometer. Raw data processing utilised the program CrysalisPro [36]. The structures were solved using direct methods and were refined against F^2 to convergence using all unique reflections and the program Shelxl [37], as implemented within WinGX [38]. For complex **3** the highly disordered structure presented is an averaged structure with a small unit cell based on a fraction of the diffraction spots. Repeated data collections on other crystals and at other temperatures did not give better data. The "true" structure may be based on a supercell of this given model or may be an incommensurately modulated structure. Attempts to model the structure in these ways failed. The averaged structure presented is used only to show the atomic connectivity of the complex generated. A recent example of the structural variation seen when modelling structures as averaged, supercell structures, or as incommensurately modulated structures is given in reference [39]. This example supports our contention that the averaged structure is proof that that the molecular structure of complex **3** is as formulated. Across the structures, many groups were found to be disordered, see deposited cif for details. Disordered groups were modelled across two sites and appropriate restraints and constraints were added to ensure that each approximated to normal geometry and displacement behaviour. Selected crystallographic and refinement parameters are given in Table S1 and full information in cif format has been deposited with the CCDC as reference numbers 2377716 to 2377723.

4.2. Synthesis of $Mg(C{\equiv}CC_6H_4Me\text{-}p)_2(THF)_4$ (1)

n-Butyl-*s*-butyl-magnesium (0.7 M in hexane, 1.42 mL, 1 mmol) was added dropwise to a solution of 4-methylphenylacetylene (0.250 ml, 2 mmol) dissolved in dry THF (5 ml) forming a yellow solution which was stirred for 2 h. The solution was cooled to −20 °C overnight yielding colourless needle-like crystals after 1 week (0.076 g, 0.140 mmol, 28 %).

^1H NMR (THF-d_8): $\delta = 7.06$ (4H, d, $^2J_{H\text{-}H} = 8.09$ Hz, C_{Ar}), 6.88 (4H, d, $^2J_{H\text{-}H} = 7.77$ Hz, C_{Ar}), 2.22 (6H, s, $CH_3 \times 2$).

^{13}C NMR (THF-d_8): δ = 133.9 (C-*C*≡C), 131.5 (C_{Ar}), 129.3 (*C*-CH_3), 128.7 (C_{Ar}), 127.6 (*C*-C≡C), 108.6 (C-C≡*C*), 21.0 (CH_3).

4.3. Synthesis of $Mg(C{\equiv}CC_6H_4CF_3\text{-}p)_2(THF)_4$ (2)

n-Butyl-*s*-butyl-magnesium (0.7 M in hexane, 4.23 ml, 3 mmol,) was added dropwise to a solution of 4-trifluoromethylphenylacetylene (0.97 ml, 6 mmol) dissolved in dry THF (5 ml) forming a colourless solution which was stirred overnight. The solution was cooled to −36 °C yielding colourless needle like crystals after 2 days (1.514 g, 2.32 mmol, 78 %).

^1H NMR (THF-d_8): δ = 7.39 (4H, d, $^2J_{H\text{-}H}$ = 8.13 Hz, CH_{meta}), 7.30 (4H, d, $^2J_{H\text{-}H}$ = 7.77 Hz, CH_{ortho}).

^{13}C NMR (THF-d_8): δ = 139.4 (C-*C*≡C), 134.5 (*C*-C≡C), 131.7 (C_{ortho}), 126.1 (*C*-CF_3, q, $^2J_{C\text{-}F}$ = 32.07 Hz), 125.6 (CF_3, q, $^1J_{C\text{-}F}$ = 271.38 Hz), 125.0 (C_{meta}, q, $^3J_{C\text{-}F}$ = 3.85 Hz), 108.1 (C-C≡*C*).

^{19}F NMR (THF-d_8): δ = −62.94.

4.4. Synthesis of $Mg(N{=}C{=}CPh_2)_2(THF)_4$ (3)

n-Butyl-*s*-butyl-magnesium (0.7 M in hexane, 7.15 ml, 5 mmol,) was added dropwise to a solution of diphenylacetonitrile (1.93 g, 10 mmol) dissolved in dry THF (5 ml) forming a colourless solution which was stirred for 2 days resulting in a green precipitate in a green solution. THF (10 ml) was added to the suspension to give a celtic green solution which upon cooling to 5 °C yielded pale green needle-like crystals after 2 days (1.121 g, 1.6 mmol, 32 %).

^1H NMR (THF-d_8): δ = 7.26 (8H, dd, $^2J_{H\text{-}H}$ = 7.25 Hz, CH_{ortho}), 7.00 (8H, t, $^3J_{H\text{-}H}$ = 7.26 Hz, CH_{meta}), 6.56 (4H, tt, $^2J_{H\text{-}H}$ = 7.24 Hz, CH_{para})

^{13}C NMR (THF-d_8): δ = 144.6 (C_{ipso}), 143.9 (*C*=N), 128.3 (C_{meta}), 123.0 (C_{ortho}), 118.4 (C_{para}), 53.2 (C-*C*=C).

4.5. Synthesis of $Mg_3(N{=}CPh_2)_4nBu_2(THF)_2$ (4)

n-Butyl-*s*-butyl-magnesium (0.7 M in hexane, 7.15 ml, 5 mmol) was added dropwise to a solution of benzophenoneimine (1.68 ml, 10 mmol) dissolved in dry THF (5 ml) forming a colourless solution and stirred for 1 h resulting in a red precipitate in a red solution. THF (10 ml) was added to the suspension making a red solution which was cooled to −20 °C yielding yellow plate-like crystals after 5 days (1.44 g, 1.37 mmol, 82 %).

^1H NMR (THF-d_8): $\delta = 7.32$ (16H, m, CH_{Ar}), 7.26 (24H, m, CH_{Ar}), 0.72 (4H, m, CH_2), 0.60 (4H, m, CH_2), 0.54 (6H, t, $^3J_{H\text{-}H} = 8.49$ Hz, CH_3), −1.24 (4H, m, Mg-CH_2).

^{13}C NMR (THF-d_8): $\delta = 176.5$ (*C*=N), 146.8 (C_{ipso}), 128.9 (C_{Ar}), 128.7 (C_{Ar}), 128.3 (C_{Ar}), 32.9 (CH_2), 32.3 (CH_2), 14.2 (CH_3), 10.7 (Mg-CH_2).

4.6. Synthesis of $(Ph_2C{=}N)_2Mg_2Cl_2(THF)_3$ (5)

BuMgCl (2.0 M in THF, 5 ml, 10 mmol) was added dropwise to a

solution of benzophenoneimine (1.68 ml, 10 mmol) dissolved in dry THF (10 ml) forming a red solution, which was next heated to 65 °C and slowly cooled in an oil bath yielding red needle like crystals overnight (2.570 g, 3.69 mmol, 74 %).

^{1}H NMR (THF-d$_8$): $\delta = 7.60$ (8H, d, $^{3}J_{H\text{-}H} = 6.22$ Hz CH_{Ar}), 7.30 (12H, m, CH_{Ar}).

^{13}C NMR (THF-d$_8$): $\delta = 173.9$ (*C*=N), 145.6 (C_{ipso}), 128.6 (C_{Ar}), 128.5 (C_{Ar}), 128.3 (C_{Ar}).

4.7. Synthesis of $[(p\text{-}FC_6H_4)_2C{=}N]_2Mg_2Br_2(THF)_3$ (6)

p-FC_6H_4MgBr (2 M in THF, 1 ml, 2 mmol) was added dropwise to a solution of *p*-fluorobenzonitrile (0.27 ml, 2 mmol) dissolved in dry THF (10 ml) forming a red solution, this was then heated to 65 °C and slowly cooled in an oil bath yielding red needle like crystals overnight (0.650 g, 0.758 mmol, 76 %).

^{1}H NMR (THF-d$_8$): $\delta = 7.64$ (2H, t, $^{3}J_{H\text{-}H} = 6.28$ Hz, CH_{Ar}), 7.08 (2H, t, $^{3}J_{H\text{-}H} = 8.66$ Hz, CH_{Ar}).

^{13}C NMR (THF-d$_8$): $\delta = 172.3$ (N=C) 164.9 (C-F), 141.7 (C_{ipso}), 130.5 (C_{Ar}), 115.3 (C_{Ar}, d, $^{2}J_{C\text{-}F} = 21.32$ Hz).

^{19}F NMR (THF-d$_8$): δ = −114.12.

4.8. Synthesis of $[(p\text{-}FC_6H_4)(o\text{-}FC_6H_4)C{=}N]_2Mg_2Br_2(THF)_3$ (7)

p-FC_6H_4MgBr (2 M in THF, 1 ml, 2 mmol) was added dropwise to a solution of *o*-fluorobenzonitrile (0.27 ml, 2 mmol) dissolved in dry THF (10 ml) forming an orange solution, which was then heated to 65 °C and slowly cooled in an oil bath before pentane was slowly diffused in overnight yielding colourless block crystals (0.310 g, 0.362 mmol, 36 %).

^{1}H NMR (THF-d$_8$): $\delta = 7.84$ (2H, br, H2), 7.60 (1H, br, H10), 7.37 (1H, m, $^{3}J_{H\text{-}H} = 5.93$ Hz, H8), 7.27 (1H, t, $^{3}J_{H\text{-}H} = 7.30$ Hz, H9), 7.11 (3H, t, $^{3}J_{H\text{-}H} = 8.09$ Hz, H3 and H7).

^{13}C NMR (THF-d$_8$): $\delta = 167.1$ (N=C), 163.7 (d, $^{1}J_{C\text{-}F} = 247$ Hz, C-F), 158.8 (d, $^{1}J_{C\text{-}F} = 243$ Hz, C-F), 137.9 (C1), 133.9 (d, $^{2}J_{C\text{-}F} = 19.6$ Hz, C5), 130.1 (br, C10), 129.4 (d, $^{3}J_{C\text{-}F} = 7.9$ Hz, *C*2), 129.1 (d, $^{3}J_{C\text{-}F} = 7.4$ Hz, C8), 125.0 (C9), 114.9 (d, $^{2}J_{C\text{-}F} = 22.3$ Hz, C7), 114.7 (d, $^{2}J_{C\text{-}F} = 21.3$ Hz, C3).

^{19}F NMR (THF-d$_8$): δ = −113.30, −117.32 (br d).

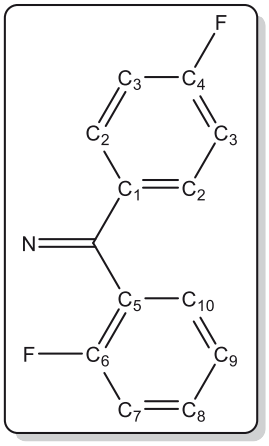

4.9. Synthesis of $Mg_3(N{=}CPh_2)_6(THF)_2{\cdot}PhMe$ (8)

n-butyl-*s*-butyl-magnesium (0.7 M in hexane, 7.15 ml, 5 mmol) was added dropwise to a solution of benzophenoneimine (1.68 ml, 10 mmol) dissolved in dry toluene (5 ml) forming a red solution, which was then heated to 100 °C and slowly cooled in an oil bath yielding red needle like crystals overnight (0.96 g, 0.77 mmol, 44 %).

^{1}H NMR (THF-d$_8$): $\delta = 7.24$ (24H, br s C_{Ar}), 7.19 (2H, toluene C_{Ar}), 7.17 (1H, toluene C_{Ar}), 7.13 (2H, toluene C_{Ar}), 7.08 (36H, m, 2 × C_{Ar}), 2.31 (3H, s, toluene CH_3).

^{13}C NMR (THF-d$_8$): $\delta = 177.0$ (*C*=N), 146.2 (C_{ipso}), 129.5 (tol), 128.7 (CH_{Ar}), 128.0 (2 x CH_{Ar}) 125.8 (tol), 21.3 (tol CH_3).

CRediT authorship contribution statement

Annabel Rae: Investigation, Formal analysis. **Alan R. Kennedy:** Validation, Data curation. **Stuart D. Robertson:** Writing – original draft, Visualization, Supervision, Funding acquisition, Conceptualization.

Declaration of competing interest

The authors declare that they have no known competing financial interests or personal relationships that could have appeared to influence the work reported in this paper.

Acknowledgements

We thank the University of Strathclyde for a PhD studentship (AR) through the Strathclyde Centre for Doctoral Training and Dr John Parkinson for help with variable temperature NMR spectroscopy.

Appendix A. Supplementary data

CCDC 2377716–2377723 contains the supplementary crystallographic data for complexes **1**–**8**. These data can be obtained free of charge via https://www.ccdc.cam.ac.uk/conts/retrieving.html, or from the Cambridge Crystallographic Data Centre, 12 Union Road, Cambridge, CB2 1EZ, UK; fax (+44) 1223-336-033; or deposit@ccdc.cam.ac.uk. The data that supports the findings of this study are available from the University of Strathclyde KnowledgeBase at https://doi.org/10.15129/588aa340-034e-48a4-a3f5-48b54d061f35. Supplementary data to this article can be found online at https://doi.org/10.1016/j.poly.2024.117257.

References

[1] S.A. Brown, S.A. Cussen, R. Kennard, S. Marchesini, J.J. Pryke, A. Rae, S. D. Robertson, R.N. Samajdar, A.J. Wain, Atom-efficient synthesis of a benchmark electrolyte for magnesium battery applications, Chem. Commun. 58 (2022) 12070–12073.

[2] N. Pour, Y. Gofer, D.T. Major, D. Aurbach, Structural analysis of electrolyte solutions for rechargeable Mg batteries by stereoscopic means and DFT calculations, J. Am. Chem. Soc. 133 (2011) 6270–6278.

[3] C. You, X. Wu, X. Yuan, Y. Chen, L. Liu, Y. Zhu, L. Fu, Y. Wu, Y.-G. Guo, T. van Ree, Advances in rechargeable Mg batteries, J. Mater. Chem. A 8 (2020) 25601–25625.

[4] Q. Sun, S. Luo, R. Huang, S. Yan, X. Lin, Recent progress of magnesium electrolytes for rechargeable magnesium batteries, Coord. Chem. Rev. 515 (2024) 215956.

[5] M. Arrowsmith, M.R. Crimmin, M.S. Hill, S.L. Lomas, D.J. MacDougall, M. F. Mahon, Catalytic and stoichiometric cumulene formation within dimeric group 2 acetylides, Organometallics 32 (2013) 4961–4972.

[6] R.J. Schwamm, M.P. Coles, Catalytic C-C bond formation promoted by organo- and amidomagnesium(II) compounds, Organometallics 32 (2013) 5277–5280.

[7] L.F. Tietze, C.A. Vock, I.K. Krimmelbein, J.M. Wiegand, L. Nacke, T. Ramachandar, K.M.D. Islam, C. Gatz, Synthesis of novel structurally simplified estrogen analogues, Chem. Eur. J. 14 (2008) 3670–3679.

[8] I.L. Fedushkin, A.G. Morozov, V.A. Chudakova, G.K. Fukin, V.K. Cherkasov, Magnesium(II) complexes of the dpp-BIAN radical-anion: synthesis, molecular structure, and catalytic activity in lactide polymerization, Eur. J. Inorg. Chem. (2009) 4995–5003.

[9] I.L. Fedushkin, A.G. Morozov, O.V. Rassadin, G.K. Fukin, Addition of nitriles to alkaline earth metal complexes of 1,2-Bis[(phenyl)imino]acenaphthenes, Chem. Eur. J. 11 (2005) 5749–5757.

[10] C. Weetman, M.D. Anker, M. Arrowsmith, M.S. Hill, G. Kociok-Köhn, D.J. Liptrot, M.F. Mahon, Magnesium-catalysed nitrile hydroboration, Chem. Sci. 7 (2016) 628–641.

[11] M. Uzelac, D.R. Armstrong, A.R. Kennedy, E. Hevia, Understanding the subtleties of frustrated lewis pair activation of carbonyl compounds by N-heterocyclic carbene/alkyl gallium pairings, Chem. Eur. J. 22 (2016) 15826–15833.

[12] V.A. Pollard, M.-A. Fuentes, S.D. Robertson, C. Weetman, A.R. Kennedy, J. Brownlie, F.J. Angus, C. Smylie, R.E. Mulvey, Reactivity studies and structural outcomes of a bulky dialkylaluminium amide in the presence of the *N*-heterocyclic carbene, ItBu, Polyhedron 209 (2021) 115469.

[13] D. Barr, W. Clegg, R.E. Mulvey, R. Snaith, Crystal structures of $(Ph_2C{=}NLi{\cdot}NC_5H_5)_4$ and $ClLi{\cdot}O{=}P(NMe_2)_3]_4$; discrete tetrameric pseudo-cubane clusters with bridging of Li_3 triangles by nitrogen and by chlorine atoms, J. Chem. Soc. Chem. Commun. (1984) 79–80.
[14] D. Barr, W. Clegg, R.E. Mulvey, R. Snaith, X-ray crystal structure of $\{Li{\cdot}[O{=}P(NMe_2)_3]_4\}^+{\cdot}\{Li_5[N{=}CPh_2]_6{\cdot}[O{=}P(NMe_2)_3]\}^-$: a lithium 'ate complex, with a pentanuclear Li_5 clustered-anion having both μ_2 edge and μ_3 face nitrogen to lithium bonding, J. Chem. Soc. Chem. Commun. (1984) 226–227.
[15] D. Barr, W. Clegg, R.E. Mulvey, R. Snaith, K. Wade, Bonding implications of interatomic distances and ligand orientations in the imino-lithium hexamers $[LiN{=}C(Ph)Bu^t]_6$ and $[LiN{=}C(Ph)NMe_2]_6$: a stacked-ring approach to these and related oligomeric organolithium systems, J. Chem. Soc. Chem. Commun. (1986) 295–297.
[16] D.R. Armstrong, D. Barr, R. Snaith, W. Clegg, R.E. Mulvey, K. Wade, D. Reed, The ring-stacking principle in organolithium chemistry: its development through the isolation and crystal structures of hexameric iminolithium clusters $(RR'C{=}NLi)_6$ (R' = Ph, R = Bu^t or Me_2N; R = R' = Me_2N or Bu^t), J. Chem. Soc. Dalton Trans. (1987) 1071–1081.
[17] J. Zhou, L.L. Liu, L.L. Cao, D.W. Stephan, Reductive coupling and loss of N_2 from magnesium diazomethane derivatives, Chem. Eur. J. 24 (2018) 8589–8595.
[18] R. Forret, A.R. Kennedy, J. Klett, R.E. Mulvey, S.D. Robertson, Multistep self-assembly of heteroleptic magnesium and sodium-magnesium benzamidinate complexes, Organometallics 29 (2010) 1436–1442.
[19] V. Semeniuchenko, S.A. Johnson, Monoanionic quasi-imido ligands based on 1-methyl-4-iminopyridine and complexes with the main group elements Mg, Al, and Zn, Organometallics 42 (2023) 769–779.
[20] W. Clegg, S.H. Dale, D.V. Graham, R.W. Harrington, E. Hevia, L.M. Hogg, A. R. Kennedy, R.E. Mulvey, Structural variations in bimetallic sodium-magnesium and sodium-zinc ketimides, and a sodium-zinc-alkide-alkoxide-amide:connections to ring-stacking, ring-laddering, and inverse crown concepts, Chem. Commun. (2007) 1641–1643.
[21] M.M. Olmstead, W.J. Grigsby, D.R. Chacon, T. Hascall, P.P. Power, Reactions between primary amines and magnesium or zinc dialkyls: intermediates in metal imide formation, Inorg. Chim. Acta 251 (1996) 273–284.
[22] E. Hollink, P. Wei, D.W. Stephan, Homoleptic magnesium bis-phosphinimide derivatives, Can. J. Chem. 83 (2005) 430–434.
[23] A.R. Kennedy, R.E. Mulvey, S.D. Robertson, N-Heterocyclic carbene stabilized adducts of alkyl magnesium amide, bisalkyl magnesium and Grignard reagents: trapping oligomeric organo s-block fragments with NHCs, Dalton Trans. 39 (2010) 9091–9099.
[24] W. Schlenk, W. Schlenk, Über die Konstitution der Grignardschen Mgnesiumverbindungen, Ber. Dtsch. Chem. Ges. B 62 (1929) 920–924.
[25] D. Seyferth, The Grignard reagents, Organometallics 28 (2009) 1598–1605.
[26] C.G. Swain, The mechanism of addition of Grignard reagents to nitriles, J. Am. Chem. Soc. 69 (1947) 2306–2309.
[27] J. Yang, P. Ruan, W. Yang, X. Feng, X. Liu, Enantioselective carben insertion into the N-H bond of benzophenone imine, Chem. Sci. 10 (2019) 10305–10309.
[28] A.B. Charette, A. Gagnon, F. Belanger-Gariepy, (*Z*)-Bis{μ-[1-(2-naphthylmethyloxy)propan-2-iminato-*O*, N:N]}bis[bromobis(tetrahydrofuran-O) magnesium] ditoluene solvate, Acta Cryst. C 56 (2000) 538–540.
[29] T. Roth, H. Wadepohl, E. Clot, L.H. Gade, Azaphilic versus carbophilic coupling at C=N bonds: key steps in titanium-assisted multicomponent reactions, Chem. Eur. J. 21 (2015) 18730–18738.
[30] A.S. Batsanov, P.D. Bolton, R.C.B. Copley, M.G. Davidson, J.A.K. Howard, C. Lustig, R.D. Price, The metallation of imino(triphenyl)phosphorane by ethylmagnesium chloride: The synthesis, isolation and X-ray structure of $[Ph_3P{=}NMgCl{\cdot}O{=}P(NMe_2)_3]_2$, J. Organomet. Chem. 550 (1998) 445–448.
[31] M. Buděšinsky, O. Exner, Correlation of carbon-13 substituent induced chemical shifts revisited: *meta*- and *para*-substituted benzonitriles, Magn. Res. Chem. 27 (1989) 27–36.
[32] R. He, Z.-T. Huang, Q.-Y. Zheng, C. Wang, Manganese-catalyzed dehydrogenative [4+2] annulation of N-H imines and alkynes by C-H/N-H activation, Angew. Chem. Int. Ed. 53 (2014) 4950–4953.
[33] A. Zweig, R.G. Fischer, J.E. Lancaster, New method for selective monofluorination of aromatics using silver difluoride, J. Org. Chem. 45 (1980) 3597–3603.
[34] M.T. Huggins, T. Kesharwani, J. Buttrick, C. Nicholson, Variable temperature NMR experiment studying restricted bond rotation, J. Chem. Educ. 97 (2020) 1425–1429.
[35] R.M. Peltzer, O. Eisenstein, A. Nova, M. Cascella, How solvent dynamics controls the Schlenk equilibrium of Grignard reagents: a computational study of CH_3MgCl in tetrahydrofuran, J. Phys. Chem. B 121 (2017) 4226–4237.
[36] Rigaku Oxford Diffraction Ltd., *CrysalisPRO*, (2016), Yarnton, England.
[37] G.M. Sheldrick, Crystal structure refinement with SHELXL, Acta Cryst. C 71 (2015) 3–8.
[38] L.J. Farrugia, WinGX and ORTEP for Windows: an update, J. Appl. Cryst. 45 (2012) 849–854.
[39] K.M. Sanders, S.K. Bruffy, A.R. Buller, V. Petříček, I.A. Guzei, Occupational modulation in the (3+1)-dimensional incommensurate structure of (2*S*,3*S*)-2-amino-3-hydroxy-3-methyl-4-phenoxybutanoic acid dihydrate, Acta Cryst. C 80 (2024) 523–533.